Inorganic Chemistry

Communication

pubs.acs.org/IC

Difluorodioxophosphate-Based Hollow Hexanuclear Lanthanide(III) Clusters Decorated with Tetrathiafulvalene Ligands

Tamyris T. da Cunha,[†,‡] Fabrice Pointillart,*[,†] Boris Le Guennic,[†] Cynthia L. M. Pereira,[‡] Stéphane Golhen,[†] Olivier Cador,[†] and Lahcène Ouahab[†]

[†]Institut des Sciences Chimiques de Rennes, UMR 6226 CNRS, Université de Rennes 1, 263 Avenue du Général Leclerc, 35042 Rennes Cedex, France

[‡]Departamento de Química, Instituto de Ciências Exatas, Universidade Federal de Minas Gerais, 31270-901 Belo Horizonte, MG, Brazil

Supporting Information

ABSTRACT: The galvanostatic reaction of the [4,5-bis(2-pyridyl-*N*-oxidemethylthio)]-4′,5′-methyldithiotetrathiafulvalene ligand with lanthanide ions in the presence of hexafluorophosphate (PF_6^-) anions afforded the highest-nuclearity lanthanide clusters decorated by tetrathiafulvalene-based ligands thanks to the original partial hydrolysis of the PF_6^- anions in difluorodioxophosphate ($PO_2F_2^-$) bridging ligands.

Coordination complexes involving lanthanide ions have been the focus of attention of the molecular magnetism community for more than a decade.[1] This activity is motivated by their ability to provide remarkable structural and physical properties such as porosity,[2] luminescence,[3] and single-molecule magnetism (SMM).[4] To design such compounds, the choice of the ligand remains crucial because (i) from a spectroscopic point of view, the efficient emission of 4f ions is sensitized thanks to the irradiation of $\pi-\pi^*$ or charge-transfer (CT) transitions of the coordinated ligands[5] and (ii) from a magnetic point of view, SMM behavior is observed with the combination of a large magnetic moment and uniaxial magnetic anisotropy.[6] The latter highly depends on the crystal-field splitting of the ground-state multiplet *J*, which is governed by the arrangement of the ligands around the lanthanide ion.

Recently, we have isolated a series of dinuclear complexes of Dy^{III} and Yb^{III} ions with [4,5-bis(2-pyridyl-*N*-oxidemethylthio)]-4′,5′-ethylenedithiotetrathiafulvene and [4,5-bis(2-pyridyl-*N*-oxidemethylthio)]-4′,5′-methyldithiotetrathiafulvene (**L**) ligands and probed their emissive and magnetic properties.[7] In these systems, the tetrathiafulvene (TTF)-based ligands **L** are neutral but act as both efficient antenna to sensitize the luminescence and structuring agents to promote the SMM behavior. To further conduct this chemistry, we present herein an alternative and original method to synthesize high-nuclearity complexes combining lanthanide ions in high symmetry (D_{4d} and C_{4v}) and neutral ligands **L**.

The galvanostatic oxidation (I = 1.5 μA) of a CH_2Cl_2/*n*-hexane (1:1 by volume) solution of $Ln(hfac)_3{\cdot}2H_2O$ ($hfac^-$ = 1,1,1,5,5,5-hexafluoroacetylacetonate; Ln = Dy^{III} and Yb^{III}), **L**, and $TBAPF_6$ (TBA = tetrabutylammonium) led to the isolation of orange crystals in stick form in both anode and cathode compartments over 4−5 days [see the Supporting Information (SI) for details]. Two novel isostructural hexanuclear lanthanide clusters of the general formula $Ln_6(PO_2F_2)_{12}(OH)_8(\mathbf{L})_2$ [Ln = Dy (**1**) and Yb (**2**)] were identified. The key step for the formation of such hexanuclear complexes is the hydrolysis of hexafluorophosphate (PF_6^-) in difluorodioxophosphate ($PO_2F_2^-$) anions. This partial hydrolysis is surprising and remarkable because such behavior was previously observed only using ionic liquids,[8] while in an aqueous solution over a long period of time, a complete hydrolysis in H_2PO_4 could only be observed.[9] Hydrolysis of the phosphate ion is very slow even in concentrated acid upon warming[9c] and even slower in basic conditions.[9d] Obviously, the coordination chemistry of this anion is almost unexplored[10] and totally unknown in the case of lanthanide ions. The presence of fluoride was confirmed by energy-dispersive spectrometry (EDS) analysis from single crystals of the compounds (Figure S1 in the SI). The metal seems to not affect the hydrolysis, while the presence of water molecules from the solvent and metal precursors is primordial. Moreover, the hydrolysis seems to overcome oxidation of the TTF fragments because the latter remain neutral in the hexanuclear complexes.

Compounds **1** and **2** (**1** is shown in Figure 1, and the perspective views of both compounds are depicted in Figures S2 and S3 in the SI) crystallize in the monoclinic space group *C*2/*c* (No. 15) (Table S1 in the SI), with the asymmetric unit containing the half-cluster. The entire molecule is generated by

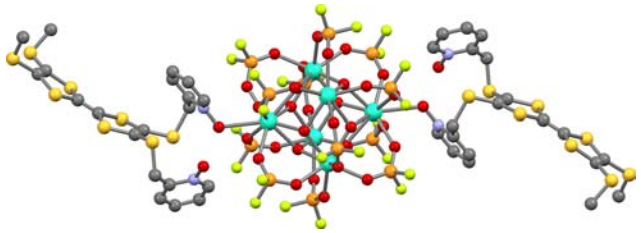

Figure 1. Molecular structure of **1**. H atoms and CH_2Cl_2 solvent molecules of crystallization are omitted for clarity. Only the F atoms with the highest occupancy are represented for clarity. Color code: Dy^{III}, light blue; O, red; N, blue; C, gray; S, yellow; F, light green. See Figures S2 and S3 in the SI for the thermal ellipsoids.

Received: May 22, 2013
Published: August 14, 2013

an inversion center. Disordered dichloromethane molecules of crystallization were identified and removed using the *PLATON/SQUEEZE* procedure.[11] With both compounds being isostructural, only **1** is described in the following, whereas the corresponding values for **2** are given in square brackets. The complex consists of six Ln^{III} ions. The metal core may be described as an octahedron involving four coplanar Ln^{III} ions (Ln1, $Ln1^{i}$, Ln2, and $Ln2^{i}$) forming the square basis, with the distances Ln1−Ln2 = 3.884(6) [3.8200(7)] Å and Ln1−$Ln2^{i}$ = 3.884(6) [3.8417(7)] Å, while the two Ln3 and $Ln3^{i}$ ions cap the square (Figure 2). Ln1 and Ln2 are surrounded by eight O atoms

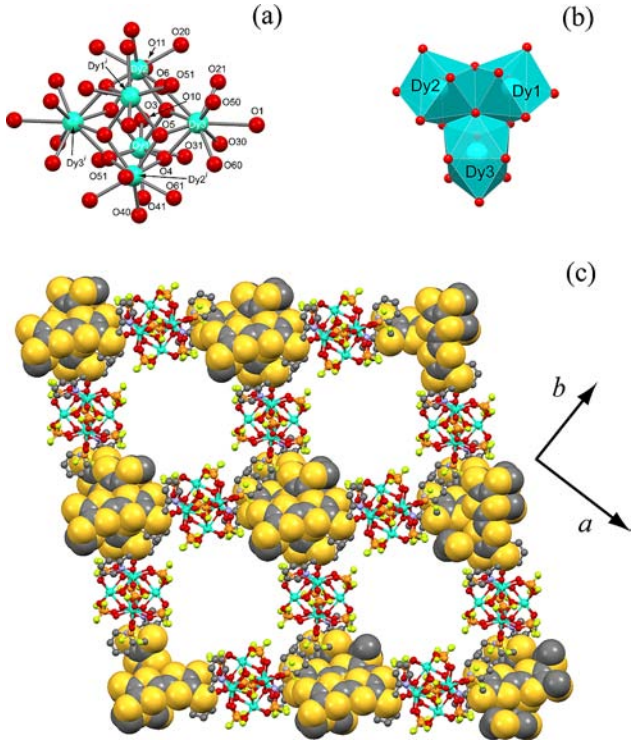

Figure 2. (a) Representation of the metal core with symmetry: i, $^3/_2 - x$, $^3/_2 - y$, $2 - z$. (b) Dy^{III} ions of the metal core with their coordination polyhedra and (c) crystal packing of **1** in the plane [110] highlighting the organic (space-filling representation) and metalloorganic (ball-and-stick representation) networks.

arising from four μ_3-OH and four μ-O_2PF_2 monoanionic bridges. Ln1 and Ln2 ions are lying in an eight-coordinated sphere of oxygen, with homogeneous Ln−O distances ranging from 2.300(6) to 2.360(5) [2.254(7)−2.322(6)] Å. Ln3 is bonded to an additional atom O1 coming from the ligand **L**. The Ln3−O distances are less homogeneous because those involving μ_3-OH^- and $PO_2F_2^-$ are in the range 2.286(6)−2.424(5) [2.242(7)−2.389(6)] Å, whereas Ln3−O1 is longer {2.758(5) [2.827(7)] Å (Table S2 in the SI)}. This last Ln3−O distance is much longer than the usual bond length involving such lanthanides and 2-pyridine-*N*-oxide acceptors.[7,12] Shape analysis unambiguously demonstrates that both eight- and nine-vertex polyhedra are close to square antiprism and capped square antiprism, respectively (Table S3 in the SI).

It is worth noting that a growing number of clusters have been seen to encapsulate anions such as carbonate[13] or oxide,[14] whereas in the present case, the metal core remains empty.[15] This is probably due to its dianionic character, while the previously described systems, in which an anion is encapsulated, display a cationic metal core. The neutrality of the complex is ensured by protonation of the remaining free pyridine-*N*-oxide acceptors. Both protonation and coordination similarly affect the *N*-oxide distances, and thus they have similar bond lengths with N1−O1 = 1.356(9) [1.352(10)] Å and N2−O2 = 1.367(10) [1.354(12)] Å. These distances are shorter than the N−O distances in the X-ray structure of the nonprotonated **L** [1.313(3) Å][7] attesting to protonation of the pyridine-*N*-oxide moiety of **L** in **1** and **2**. Considering this fact, each ligand **L** is monocationic; nevertheless, the central C5═C6 bond lengths {1.363(11) [1.327(13)] Å} attest to the neutral form of the TTF core. Dimers of donor **L** are formed through S3···S4 short contacts. A monodimensional organic network is generated by additional S3···S4 and S6···S6 lateral short contacts, and the metalloorganic network is formed by the Ln_6 clusters (Figures 2c and S4 in the SI). Figure 2c illustrates the crystal packing of **1** in the [110] plane and highlights the formation of a three-dimensional molecular grid with squared channels along the *c* axis (Figure S5 in the SI). The empty channels have an approximate diameter of 14.8 × 13.7 Å. The pillars of the three-dimensional grid are formed by the one-dimensional organic networks, while the linkers between the pillars are represented by the metal core (Figure 2c).

The redox properties of **L** and the related complexes **1** and **2** were investigated by cyclic voltammetry (Figure S6 and Table S4 in the SI). The cyclic voltammograms show two reversible monoelectronic oxidations at about 0.51 and 0.85 V corresponding to the formation of a TTF radical cation and a dication, respectively. An oxidation wave with weak intensity was identified at ca. 1.10 V and may be attributed to the presence of some impurities. Upon coordination to the lanthanide, both $E^1_{1/2}$ and $E^2_{1/2}$ are not significantly shifted compared with the potentials of the free ligand. This differs from the anodic shift usually observed for previous coordination complexes involving similar ligands,[7,12] but this can be easily explained by (i) the absence of the electron-attracting $hfac^-$ anions and (ii) the long Ln3−O1 bond length, which decreases the electrostatic effect of the Ln^{III} ion.[16] No duplication of the oxidation waves is observed, indicating that oxidation and reduction are simultaneous for the two ligands **L**. The electrochemical properties attest to the redox activity of **L** in the complexes.

The UV−visible absorption properties of **L** were studied in a CH_2Cl_2 solution (Figure 3a) and rationalized by time-dependent density functional theory calculations (Figures 3b and S7 in the SI).[17] The experimental absorption curve of **L** was deconvoluted into six bands (Figure 3a and Table S5 in the SI). The lowest-energy band was calculated at 23981 cm^{-1} (experimental value found at 21300 cm^{-1}, red Gaussian deconvolution) and attributed to a $\pi-\pi^*$ HOMO → LUMO TTF core to methyl-2-pyridine-*N*-oxide charge transfer (ILCT) (Figures 3a,b and Table S5 in the SI). The following absorption bands are mainly attributed to $\pi-\pi^*$ intradonor (ID) excitations, while the highest-energy band (blue deconvolution) is attributed to an intraacceptor (IA) contribution (Table S5 in the SI). The UV−visible spectrum of **1** was obtained in the solid state, which prevents dissociation of the coordination complex (Figures 3c and Table S6 in the SI). As a result, the absorption properties of the hexanuclear complexes are almost identical with those of the free ligand because the metallic core does not absorb in the studied UV−visible range.

At room temperature, the $\chi_M T$ product (χ_M being the molar susceptibility and *T* the temperature) is equal to 82.5 $cm^3\ mol^{-1}$ K for compound **1**, being consistent with the presence of six

dx.doi.org/10.1021/ic4012839 | *Inorg. Chem.* 2013, 52, 9711−9713

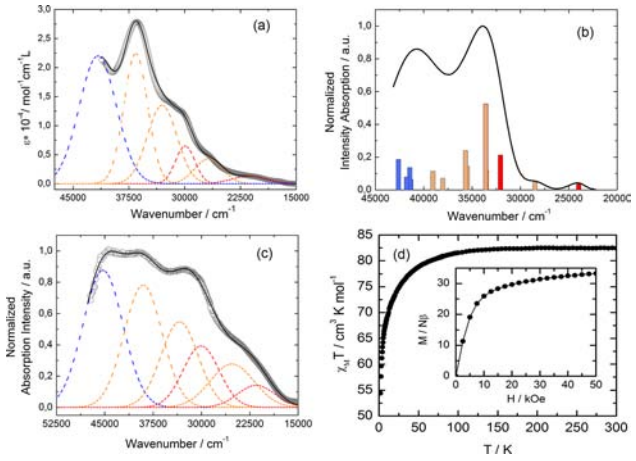

Figure 3. (a) Experimental UV−visible absorption spectra of **L** ($C = 4 \times 10^{-5}$ mol L^{-1}) in a CH_2Cl_2 solution (open gray circles), Gaussian deconvolutions (dashed lines), and a best-fit curve with six Gaussians (solid line; $R = 0.99908$). (b) Calculated UV−visible spectra of **L** (black line). The sticks represent the mean contributions of the absorption spectra for **L**. (c) Experimental UV−visible absorption spectra of **1** in the solid state (open gray circles), Gaussian deconvolutions (dashed lines), and a best-fit curve with six Gaussians (solid line; $R = 0.99948$). Color code: red, ILCT; orange, ID; blue, IA. (d) Thermal variation of $\chi_M T$ and magnetization curve versus applied field at 2 K for **1** (inset).

noninteracting Dy^{III} ($S = {}^5/_2$, $L = 5$, ${}^6H_{15/2}$, $g = {}^4/_3$, $C = 14.17$ cm^3 mol^{-1} K) centers. The $\chi_M T$ value gradually decreases upon a lowering of the temperature, being more abrupt below 40 K (Figure 3d). It can be due to depopulation of the M_J sublevels of the J ground state and to weak antiferromagnetic exchange and dipolar interactions. The magnetization curve shows a rapid increase at low fields, reaching a value of 33.28 Nβ at 2 K and 5 T (inset of Figure 3d). The possible SMM behavior was checked by solid-state alternating-current (ac) susceptibility under 0 and 1000 Oe applied fields. Unfortunately, the out-of-phase susceptibility values (χ_M'') are negligible at low temperature.

In summary, a new hexanuclear cluster of lanthanides has been prepared through the partial hydrolysis of PF_6^- anions in $PO_2F_2^-$ bridging ligands. Up to now, they are the highest-nuclearity compounds involving lanthanides and TTF ligands and are obtained through an original protocol, i.e., electrocrystallization method. The six lanthanide ions of the cluster adopt either D_{4d} or C_{4v} high symmetry in their coordination spheres. The center of the metal core of **1** does not contain any anion but instead is decorated by two redox-active TTF ligands, opening perspectives for electronic conductivity. The crystal packing reveals very large channels. Magnetic studies indicate only classical paramagnetic behavior for such polynuclear compounds. Nevertheless, this new synthetic approach opens perspectives in the elaboration of interesting lanthanide clusters.

■ ASSOCIATED CONTENT

Ⓢ Supporting Information

Experimental section, crystallographic information in CIF format, crystallographic data (Table S1), selected bond lengths (Table S2), SEM and EDS analysis for **1** (Figure S1), perspective views of **1** (Figure S2) and **2** (Figure S3), crystal packing of **1** (Figure S4), channels in **1** (Figure S5), SHAPE analysis of **1** (Table S3), cyclic voltammetry for **L**, **1**, and **2** (Figure S6 and Table S4), experimental and calculated absorption data (Tables S5 and S6), and MO diagram for **L** (Figure S7). This material is available free of charge via the Internet at http://pubs.acs.org.

■ AUTHOR INFORMATION

Corresponding Author

*E-mail: fabrice.pointillart@univ-rennes1.fr.

Notes

The authors declare no competing financial interest.

■ ACKNOWLEDGMENTS

This work was supported by the CNRS, Rennes Métropole, Université de Rennes 1, Région Bretagne, FEDER, and CNPq.

■ REFERENCES

(1) Gschneider, K. A., Bünzli, J. C. G., Pecharsky, V. K., Eds. *Handbook on the Physics and Chemistry of Rare Eaths*; Elsevier: Amsterdam, The Netherlands, 2005.

(2) (a) Devic, T.; Serre, C.; Audebrand, N.; Marrot, J.; Ferey, G. *J. Am. Chem. Soc.* **2005**, *127*, 12788. (b) Cui, Y. J.; Yue, Y. F.; Qian, G. D.; Chen, B. L. *Chem. Rev.* **2012**, *112*, 1126.

(3) (a) Binnemans, K. *Chem. Rev.* **2009**, *109*, 4283. (b) Bünzli, J. C. G.; Piguet, C. *Chem. Soc. Rev.* **2005**, *34*, 1048. (c) Bünzli, J. C. G. *Acc. Chem. Res.* **2006**, *39*, 53. (d) Eliseeva, S. V.; Bünzli, J. C. G. *Chem. Soc. Rev.* **2010**, *39*, 189. (e) Bünzli, J. C. G.; Eliseeva, S. V. *Chem. Sci.* **2013**, *4*, 1939.

(4) Woodruff, D. N.; Winpenny, R. E. P.; Layfield, R. A. *Chem. Rev.* **2013**, DOI: 10.1021/cr400018q.

(5) D'Aléo, A.; Pointillart, F.; Ouahab, L.; Andraud, C.; Maury, O. *Coord. Chem. Rev.* **2012**, *256*, 1604.

(6) Bünzli, J. C. G.; Piguet, C. *Chem. Rev.* **2002**, *102*, 1897.

(7) Pointillart, F.; Le Guennic, B.; Cauchy, T.; Golhen, S.; Cador, O.; Maury, O.; Ouahab, L. *Inorg. Chem.* **2013**, *52*, 5978.

(8) Freire, M. G.; Neves, C. M. S. S.; Marrucho, I. M.; Coutinho, J. A. P.; Fernandes, A. M. *J. Phys. Chem. A* **2010**, *114*, 3744.

(9) (a) Spiccia, L.; Graham, B.; Hearn, M. T. W.; Lazarev, G.; Moubaraki, B.; Murray, K. S.; Tiekink, E. R. T. *J. Chem. Soc., Dalton Trans.* **1997**, 4089. (b) Pope, S. J. A.; Coe, B. J.; Faulkner, S.; Laye, R. H. *Dalton Trans.* **2005**, 1482. (c) Gebala, A. E.; Jones, M. M. *J. Inorg. Nucl. Chem.* **1969**, *31*, 771. (d) Ryss, I. G.; Tulchinskii, V. B. *Zh. Neorg. Khim.* **1964**, *9*, 836.

(10) Vast, P.; Semmoud, A. *J. Therm. Anal.* **1994**, *41*, 1489.

(11) Spek, A. L. *Acta Crystallogr.* **2009**, *D65*, 148.

(12) Pointillart, F.; Le Guennic, B.; Golhen, S.; Cador, O.; Maury, O.; Ouahab, L. *Inorg. Chem.* **2013**, *52*, 1610.

(13) (a) Tian, H.; Zhao, L.; Guo, Y.-N.; Guo, Y.; Tang, J.; Liu, Z. *Chem. Commun.* **2012**, *48*, 708. (b) Tian, H.; Guo, Y.-N.; Zhao, L.; Tang, J.; Liu, Z. *Inorg. Chem.* **2011**, *50*, 8688. (c) Gass, I. A.; Moubaraki, B.; Langley, S. K.; Batten, S. R.; Murray, K. S. *Chem. Commun.* **2012**, *48*, 2089. (d) Langley, S. K.; Moubaraki, B.; Murray, K. S. *Inorg. Chem.* 10.1021/ic3002724.

(14) (a) Lin, S.-T.; Wernsdorfer, W.; Ungur, L.; Powell, A. K.; Guo, Y.-N.; Tang, J.; Zhao, L.; Chibotaru, L. F.; Zhang, H.-J. *Angew. Chem., Int. Ed.* **2012**, *51*, 12767. (b) Calvez, G.; Daiguebonne, C.; Guillou, O. *Inorg. Chem.* **2011**, *50*, 2851.

(15) (a) Mereacre, V.; Ako, A. M.; Nadeem Akhtar, M.; Lindemann, A.; Anson, C. E.; Powell, A. K. *Helv. Chim. Acta* **2009**, *92*, 2507. (b) Xiang, S.; Hu, S.; Sheng, T.; Fu, R.; Wu, X.; Zhang, X. *J. Am. Chem. Soc.* **2007**, *129*, 15144.

(16) Pointillart, F.; Cauchy, T.; Maury, O.; Le Gal, Y.; Golhen, S.; Cador, O.; Ouahab, L. *Chem.—Eur. J.* **2010**, *16*, 11926.

(17) Cosquer, G.; Pointillart, F.; Le Guennic, B.; Le Gal, Y.; Golhen, S.; Cador, O.; Ouahab, L. *Inorg. Chem.* **2012**, *51*, 8488.